INTERNATIONAL ATOMIC ENERGY AGENCY
UNITED NATIONS EDUCATIONAL, SCIENTIFIC AND CULTURAL ORGANIZATION

INTERNATIONAL CENTRE FOR THEORETICAL PHYSICS
34100 TRIESTE (ITALY) - P.O.B. 586 - MIRAMARE - STRADA COSTIERA 11 - TELEPHONE: 2240-1
CABLE: CENTRATOM - TELEX 460392 - I

SMR/390 - 6

WORKING PARTY ON "FRACTURE PHYSICS"
(29 May - 16 June 1989)

FROM DISLOCATION DYNAMICS TO SELF ORGANIZATION OF DISLOCATIONS

G. ANANTHAKRISHNA
Indira Gandhi Centre for Atomic Research
Materials Science Laboratory
603 102 Kalpakkam
India

Self Organization in Physical Systems

G. Ananthakrishna

Quite often the word organization gives an impression of ordering (at least in the physical sciences). What then is self organization ? To answer this we will start with the familiar example in thermodynamics namely the formation of water from water vapour and ice from water. This transformation of phase from one to another occurs when the temperature of the vessel containing the material (the sub system) is lowered. The temperature of the system is changed by keeping it in contact with a reservoir whose temperature can be manipulated at will. At elevated temperatures the gas molecules move freely. When the temperature is reduced below a certain temperature, the molecules are within a certain distance from each other. Motion of any molecule strongly affects the motion of the molecules in the neighbourhood. In other words, the motion of the molecules is correlated. In the solid phase, (below the freezing temperature) the molecules are arranged in a particular order. The gaseous phase in which the molecules are free to move anywhere in the vessel, is the most disordered phase of the three. In the solid phase, the molecules are more or less constrained to move between deep potential barriers (which are seperated by distances of the order 10^{-8}cm.) for which the locations are positionally ordered. Thus solid is the most ordered phase. The degree of freedom of movement is, loosely speaking, a measure of disorder. In the technical language of thermodynamics, one assigns a quantity called entropy as a measure of disorder defined by $S = K_B \ln p$, where K_B is the Boltzmann's constant, and p is the number of allowed configurations.

We consider now the transition from a ferromagnetic phase (with non-zero magnetisation) to a paramagnetic phase (with zero magnetisation) as the temperature is increased. At low temperatures, the elementary constituent magnets (spins) are aligned in one direction (with a high degree of correlations) resulting in a finite magnetic moment, whereas at high temperatures they are oriented randomly giving rise to zero magnetic moment. At high temperatures the spins behave independently of each other (or are uncorrelated). Exactly how the high degree of correlation arises (in the ordered state) between the elementary constituents (molecules, spins etc.) giving rise to the bulk properties characterising the low temperature phase of the system, is the subject of phase transition in the realm of equilibrium statistical mechanics. There are many examples of such phase transitions, wherein the low temperature phase has a non-zero value of a bulk property (magnetization for example) whereas the same property is zero in the high temperature phase. We shall call this bulk property the order parameter of the phase.

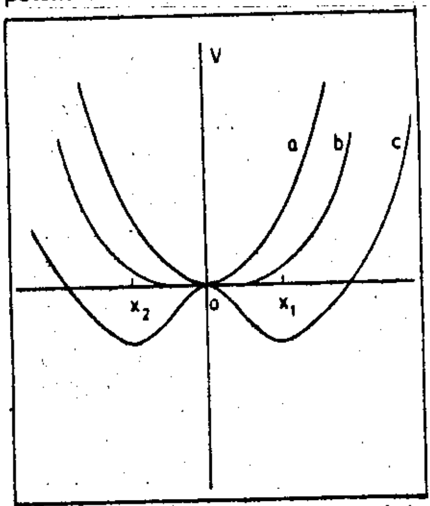

Fig. 1 Free energy as a function of the order parameter for $T > T_c$, $T \sim T_c$ and $T < T_c$.

For systems in equilibrium, the response of the system to an applied force is linear. To understand this consider a potential as shown in figure 1. (The curve marked a.) If a ball is displaced from its equilibrium position $x = 0$ by a small force, the displacement will be linear ($F \propto x$) and the ball will oscillate periodically in the absence of friction about $x = 0$. In thermodynamics the role of the potential is taken by free energy which in the high temperature phase has a single minimum at the origin of the order parameter (corresponding to zero magnetization, for example). This minimum represents a stable configuration. Any disturbance or fluctuation remains bounded. Consider the potential with the flat bottom (curve b) in figure 1. In this case, it should be clear that even a very small force can cause a very large displacement. So the response of the system is more. If we release a ball at $x \neq 0$ the ball will fall slower in case b than in case a. For the magnetic case near a temperature called the Curie temperature T_c, the free energy becomes flat and hence the response of the system becomes large and fluctuations decay slowly. This property is called critical slowing. (Compare the above mechanical analogy.) Magnetic susceptibility which is a measure of the response of the system, becomes very large as $T \rightarrow T_c$ (case b in figure 1). The last case (curve c) is the double well potential. The state when $x = 0$ is no longer stable. A ball placed at $x = 0$, with even the slightest disturbance will end up in one of the potential minima. This curve represents the free energy for $T > T_c$ where the magnetization can assume two equivalent values. Written in the Landau form, the free energy F can be expanded as

$$F = a_0' + a_1 (T - T_c)M^2 + a_2M^4 \quad (1)$$

where a_0, a_1 and a_2 are constants and M is the magnetization. The phase change basically occurs due to a competition between the internal energy U, and the entropy term in the free energy $F = U - TS$. Since the temperature of the system decides whether the system is in an ordered phase or in a disordered phase, all the ordered structures or phases are equilibrium structures.

Thermodynamics tells us that for any closed system, entropy increases reaching a maximum corresponding to the equilibrium configuration. For example, consider a vessel with a wall in between, and have some gas in one part of the vessel in equilibrium. If we remove the wall, the gas tends to occupy the whole volume for which the entropy will be larger than for the initial configuration. It never happens that all the gas molecules get concentrated back into one part of the vessel. The point to note here is that this irreversible change is due to the large number of molecules present as can be seen by the following argument. In contrast to the above case if we have only, say, three molecules, it is quite conceivable that at some later instant all the three molecules could be back in one part of the vessel. Thus a property of mechanics, namely time reversal invariance breaks down when the number of degrees of freedom is large.

In the above example a constraint (wall) was removed and the order decreased. The reverse question is, can the entropy decrease if we constrain the system appropriately ? The answer is yes, but the system will not be in equilibrium. For example, if we consider a mixture of two gases under a thermal gradient, we find that one of the gases concentrates at the hotter end and the other gas concentrates at the cooler end. The entropy of this inhomogeneous mixture will be less than the homogeneous mixture. Yet there is no ordering of this kind in the equilibrium structures that we discussed earlier. Neither is there any new macroscopic order in terms of easily recognisable spatial patterns, which are possible as we will see later if the situation is far from equilibrium.

There are many situations in daily life in which an ordered situation can arise if we supply the appropriate amount of energy from outside. For example, regular impulses to compensate for friction in a pendulum or energy supplied to an engine at regular intervals will sustain their motion. If the energy is supplied at random, the motion can not be sustained. Even in the case where periodic impulses are supplied the ordering is due to 'action from outside'. Now the question is whether there can be ordering due to natural constraints within the system ? This is possible provided we take what is called outside influence as part of the system so that we have to have a knowledge of how this outside influence evolved. Equivalently, we have to consider the influence of the subsystem on the reservoir properties also. (This should be contrasted with systems in thermodynamic equilibrium where the temperature of the system could be altered by keeping it in contact with a heat bath of infinite thermal capacity.) Obviously, if this has to happen, the subsystem will have to be moved so far away from thermal equilibrium that it starts reacting back on the properties of the reservoir, which in turn can appropriately change the magnitude of influence caused by the reservoir on the subsystem. In other words, there should be a feedback of information which acts as an autoregulatory mechanism. Under favourable conditions this can give rise to a new kind of spatial and temporal order. The initial disordered state is homogeneous in space and time.

Under the action of drive parameters such as matter, energy, fields etc., the system moves away from equilibrium. Beyond a critical value of the drive parameters, the system goes into a spatially ordered state or may become periodic in time. The resulting ordered state has an entropy less than the initial disordered homogeneous state. These transitions do bear similarities to the equilibrium phase transitions. However, there are two essential differences. The first is that these systems are intrinsically nonlinear and the other is that they are not time reversal invarient in contrast to systems in equilibrium. The formation of the new ordered state under the influence of a drive parameter is referred to as self organization, Ilya Prigogine[1] and his school refer to this new type of order as a Dissipative Structure. The study of this fascinating subject has been called as synergetics by Herman Haken[2] . Another point to note is that the ordered state is in dynamical balance. The moment the action of the drive parameter is withdrawn, the system reverts back to the equilibrium disordered state. Examples of self organized systems can be found in disciplines as varied as physics and biology. Below are some examples drawn from different disciplines. In each case an attempt is made to bring out the drive parameter, the initial disordered state and the final ordered state.

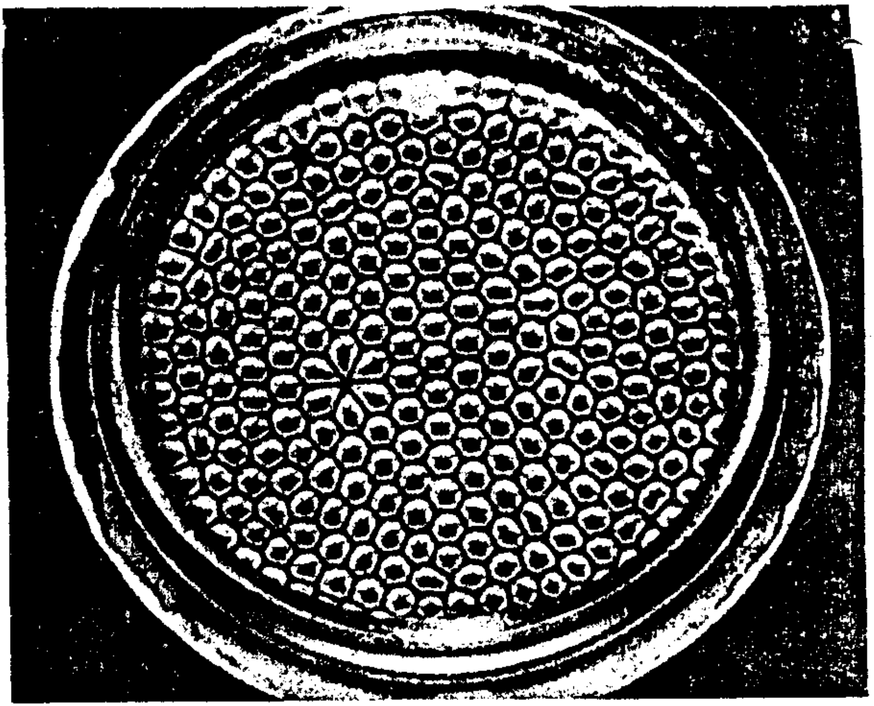

Fig. 2 Rayleigh Benard instability as seen from above.

i) Rayleigh-Benard Instability

This instability refers to heat transport changing from a conduction mode to a convective mode when a liquid kept in a dish is heated. Consider a liquid heated from below. Assume that the upper layer is held at a constant temperature T_1 which is less than T_2 of the bottom layer ($T_2 - T_1 = \Delta T$). For small ΔT, although the liquid at the bottom layer has a tendency to move up, the convective motion is prevented by the viscocity of the liquid. Heat is transported by conduction. However, for large ΔT, the input heat energy cannot be conducted away. In this case the heated parts expand and move up due to buoyancy, cooling as they rise up, thereby falling back. This gives rise to a surprisingly regular spatial pattern. All this happens beyond a critical value of ΔT. The original conduction mode becomes unstable giving way to a stable convective motion. For a circular geometry, viewed from the top, the cells arrange themselves in a honeycomb structure (see figure 2). The drive parameter in this case is in dynamic state and emerges out of a completely disordered homogeneous state. If we try to calculate the probability of occurrence of such a coherent conversion pattern involving about 10^{23} molecular via $P \sim \exp S/k_B$ it would be almost zero. Thus the convective pattern is essentially a far from equilibrium situation.

Taylor instability is another example drawn from hydrodynamics. Here the fluid is enclosed between two coaxial cylinders with the outer cylinder fixed and the inner cylinder rotating at a constant angular velocity. For low angular velocities, high angular momentum of the inner layers is transported outwards resulting in a streamline flow spiraling outwards. Beyond a threshold value of the angular velocity this state becomes unstable and macroscopic vortices appear.

ii) Belousov-Zhabotinski Oscillating Chemical Reaction [1-3]

Normally when we mix chemicals that can react to form new products, the

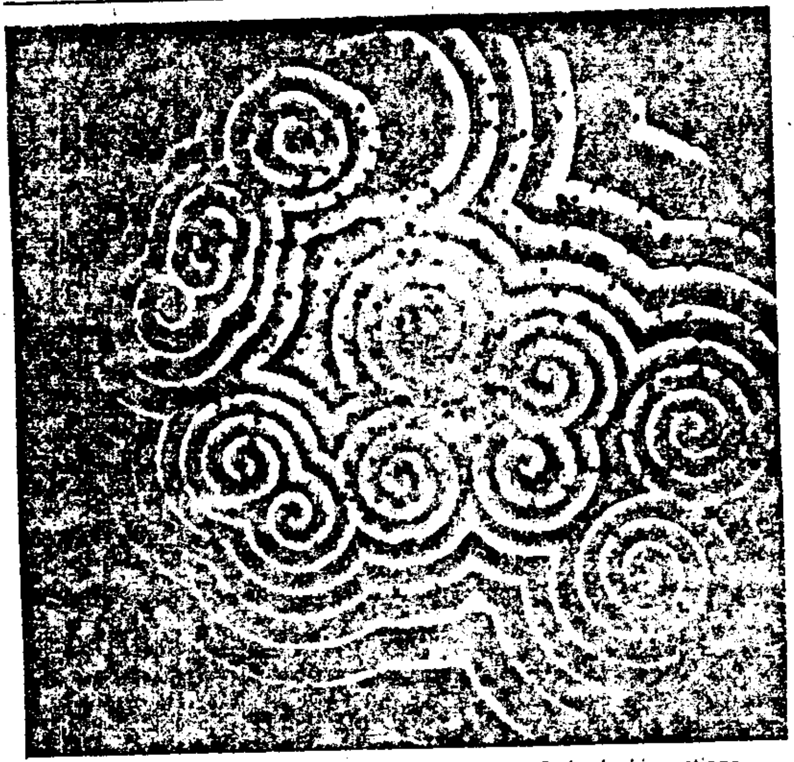

Fig. 3 Spirals of chemical activity in Belousov-Zhabotinski reactions (after A.T. Winfree).

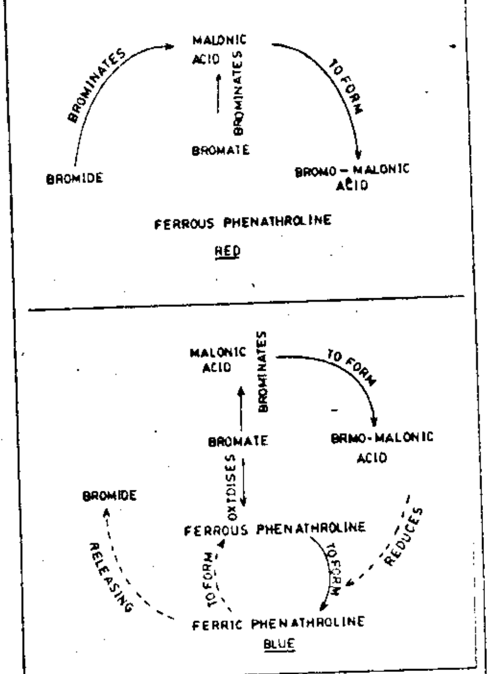

Fig. 4 The two reaction pathways in Belousov-Zhabotinski reactions (after A.T. Winfree).

concentration of various chemicals follows monotonic behaviour as a function of time. This need not always be the case. As the above name suggests, in the B-Z reaction the concentration of the chemicals oscillates in time. Belousov, who first discovered it around 1950, failed (except for a brief communication) to get the work past the referees and editors of two journals[4], since his results did not fit into the then existing theories. To begin with consider the following recipe of oscillating chemical reaction borrowed from Winfree[3]. Add 2 ml of concentrated H_2SO_4 and 5 g of sodium bromate to 67 ml of water. Transfer 6 ml of this to a petri dish to which add 1 ml of malonic acid solution (1 g per 10 ml). To this add 0.5 ml of sodium bromide solution (1 g in 10 ml) and wait for the bromine colour to vanish. Add 1 ml of 25 mM phenanthroline ferrous sulphate and a drop of triton X–100 surfactant solution (1 g in 1000 ml) to facilitate spreading. Mix well and pour the solution into a covered perti dish illuminated from below. The solution turns blue then reverts to red. This happens periodically. A variety of spatial patterns are possible (Figure 3).

The oscillatory nature of the chemical reaction can be understood by describing reactions among bromide, bromate, malonic acid and iron phenanthroline (which serves as a catalyst as well as an indicator dye). Two set of reactions are involved (indicated in figure 4). The concentration of bromide determines which reaction course is followed. The first set of reactions is followed until the bromide concentration falls below a threshold at which point the control switches to the second set of reactions. In the first set of reactions, both bromide and bromate, brominate malonic acid to form bromomalonic acid. During this time ferrous phenanthroline remains red (ie. the iron atom is in the ferrous form). When the concentration of bromide falls below a threshold value the second set of reactions starts to dominate. The last bit of bromide is consumed and then bromate takes over bromination of malonic acid. During this stage bromate oxidises ferrous phenanthroline to the ferric form which is blue in colour. Later the bromomalonic acid reduces ferric phenanthroline back to ferrous form (shown as dashed line) releasing simultaneously bromide and carbon dioxide. As the bromide concentration increases, it shuts off the second reaction and restarts the first which brings back the red colour. (Carbon dioxide can be removed by stirring every 15 minutes.)

At the time when this reaction was studied by Belousov and Zhabotinski, nobody could forsee the impact this work was going to have on the development of the subject of synergetics and dissipative structures. The richness of the model is enormous. Topologically different kinds of wave patterns have been studied. The interested reader can refer to a recent monograph by Winfree and to his other papers[3-5].

iii) Formation of Mammalian Coat Patterns

Nature is full of examples of pattern formation. For example, we notice different kinds of coat patterns in mammals. It is interesting to note that such coat patterns can be described by methods of self organization[6]. Bard[7] has evolved a mathematical model which under various initial and boundry conditions generates the complex variety of coat patterns found in mammals. The model consists of a coupled set of reactive-diffusive equations for two chemical species (two mophogens) determining the colour. The model predicts several coat patterns. Figure 5 shows theoretically generated patterns marked a, c and d corresponding to the patterns on a fallow deer, a masai giraffe and a cape giraffe. Clearly the theoretically generated patterns are very similar to the patterns found on these mammals.

Another example of pattern formation can be found in crystal growth. We just mention the formation of snow flakes and dendritic crystals[8].

iv) Repeated Yield Drop Phenomenon [9].

When a material is pulled at a constant rate, the monitored load shows a yield drop. This is schematically shown by the dashed line in figure 6. A single yield drop is what is normally observed. However, under certain conditions, ins-

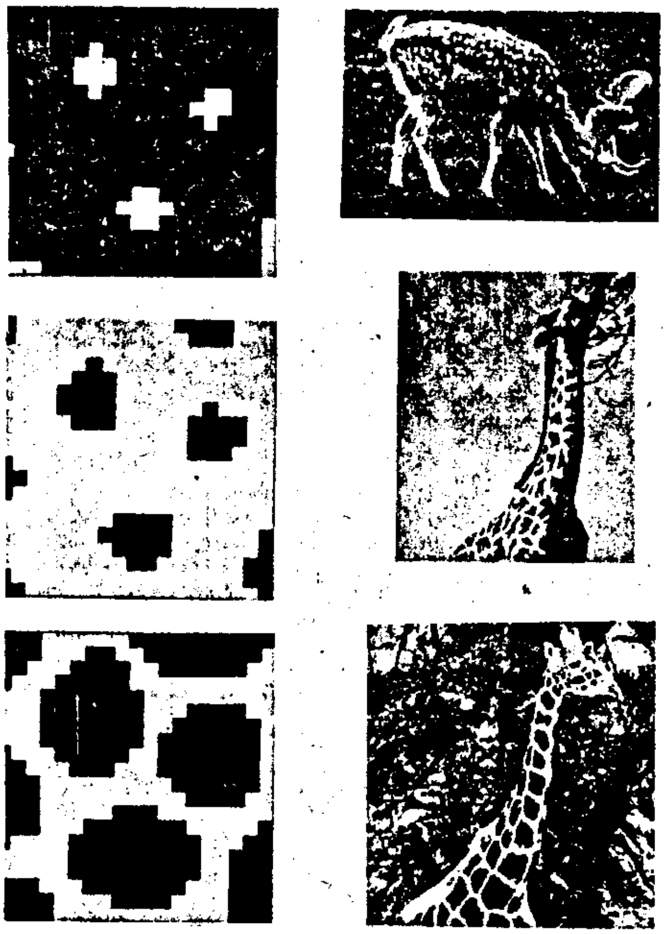

Fig. 5 Theoretically generated patterns corresponding to a fallow deer, masai giraffe and a cape giraffe. (after J.L.B. Bard)

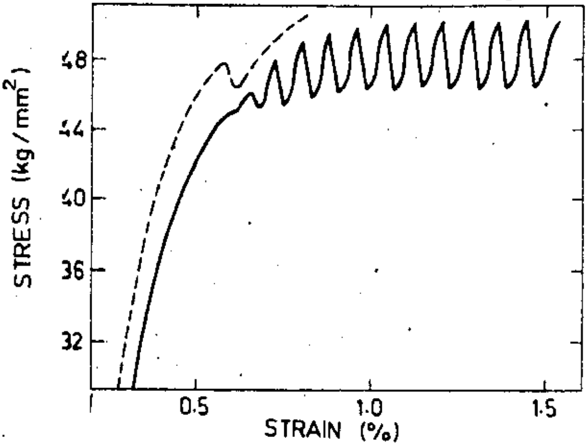

Fig. 6 Single yield drop and multiple yield drops.

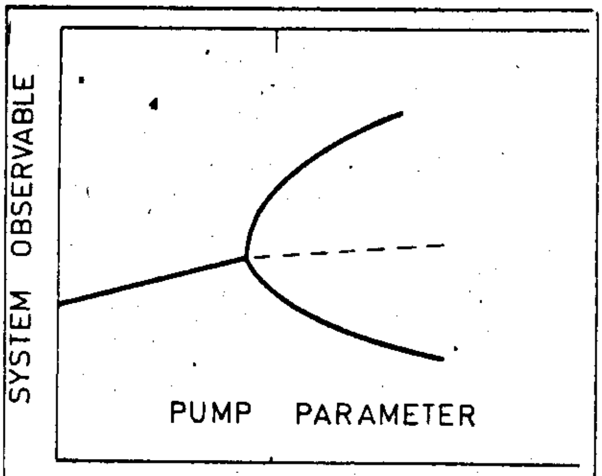

Fig. 7 Bifurcation diagram.

tead of a single yield drop, several yield drops are seen (continuous curve in figure 6). The parameters which give rise to such a change are the rate of pulling (strain rate), temperature and other metallurgical parameters. Up to a certain rate of pulling only one yield drop is seen. Beyond a critical value of strain rate, repeated yield drops are seen. Generally, the deformation is inhomogeneous when the multiple yielding is seen. Here the single yield drop which is space-time homogeneous is the disordered state, and the state of repeated yielding is the temporally ordered (and spatially inhomogeneous) state. The drive parameter is the strain rate.

In the table is listed some characteristics of the various examples which have been considered.

In all these cases, under the action of an external drive parameter, the system which may be in thermodynamic equilibrium moves away from equilibrium through a sequence of steady states connected to that equilibrium state which occurs when the drive parameter is zero. This equilibrium branch or thermodynamic branch as it is often called, can become unstable at some critical value of the drive parameter with simultaneous appearance of new states (see figure 7). This is similar to the equilibrium phase transition discussed earlier. Recall that the nature of the free energy changes from a single well shape to double well shape as we pass from T> T_c to T< T_c (see figure 1 and the relevant text). x = 0 was stable under small perturbations for T> T_c with peturbations decaying exponentially. For T< T_c, x = 0 is no longer stable to perturbations. Indeed they grow exponentially for short times. The stability of x = 0 has changed and two new steady states $X = X_1$ and $X = X_2$ arise as we change T across T_c. This qualitative change in the nature of solutions (states) of the system as a function of the drive parameter, is called bifurcation. For the sake of illustration, let us consider a simple function $f(t) = \exp \lambda t$. For $\lambda < 0$, f(t) decays as a function of time t; for $\lambda > 0$, f(t) blows up. The nature of the solution changes qualitatively as λ goes from a negative to a positive value. λ can also take on complex values and again the nature of solution changes. If λ is considered as a drive parameter, $\mathrm{Re}\,\lambda = 0$, $\mathrm{Im}\,\lambda = 0$ and $\mathrm{Re}\,\lambda = 0$, $\mathrm{Im}\,\lambda \neq 0$ are both points of bifurcation.

In many cases the bifurcation may happen, not just once but for a sequen-

Phenomenon	Disordered state	Ordered state	Drive parameter
Bernard Instability	Conduction mode	Convective mode	Temperature difference
Taylor Instability	Streamline Couette flow	Convective mode (vortices)	Angular velocity
Belousov Zhabotinski Reaction	Space-time homogeneous	Space-time inhomogeneous	Rate constants.
Repeated Yield Drops	Single Yield Drop	Multiple Yield Drops	Strain rate

ttern is realised.
lving the above
the presence of
s probabilistic ev-
ne final realised

o thank Drs. C.S. Sundar
suggestions in making

1977) Self Organization
Wiley, New York.
Springer-Verlag, Berlin.
Geometry of Biological
n.
n. Education 61 661.
ogatz (1984) Physica 130
Formation by Dynamical
nition, Springer-Verlag,
Biol. 93 363.
I. Phys. 52 1.
C. Valsakumar (1982) J.
hys. 53 655, and D.R.
245 16.

ysicist who is at pre-
e Laboratory, of the
Kalpakkam.

understand which pattern is realised. This would mean solving the above nonlinear equations in the presence of small fluctuations. Thus probabilistic evolution determines the final realised pattern.

Acknowledgement; *I would like to thank Drs. C.S. Sundar and R.V. Nandedkar for their suggestions in making the manuscript more readable.*

References

1. G.Nicolis and I. Prigogine (1977) Self Organization in Nonequilibrium Systems, Wiley, New York.
2. H. Haken (1978) Synergetics, Springer-Verlag, Berlin.
3. A.T. Winfree (1980) The Geometry of Biological Time, Springer-Verlag, Berlin.
4. A.T. Winfree (1984) J. Chem. Education 61 661.
5. A.T. Winfree and S.H. Strogatz (1984) Physica 130 247 and references therein.
6. H. Haken Ed. (1979) Pattern Formation by Dynamical Systems and Pattern Recognition, Springer-Verlag, Berlin
7. J.B.L. Bard (1981) J. Theor. Biol. 93 363.
8. J.S. Langer (1980) Rev. Mod. Phys. 52 1.
9. G. Ananthakrishna and M.C. Valsakumar (1982) J. Phys. D 15 L171.
10. E. Ott (1981) Rev. Mod. Phys. 53 655, and D.R. Hofstadter (1981) Sci. Am. 245 16.

G. Anantha Krishna is a Physicist who is at present in the Materials Science Laboratory, of the Reactor Research Centre, Kalpakkam.

NON LINEAR PHENOMENA
IN
MATERIALS SCIENCE

AUSSOIS - FRANCE
1987

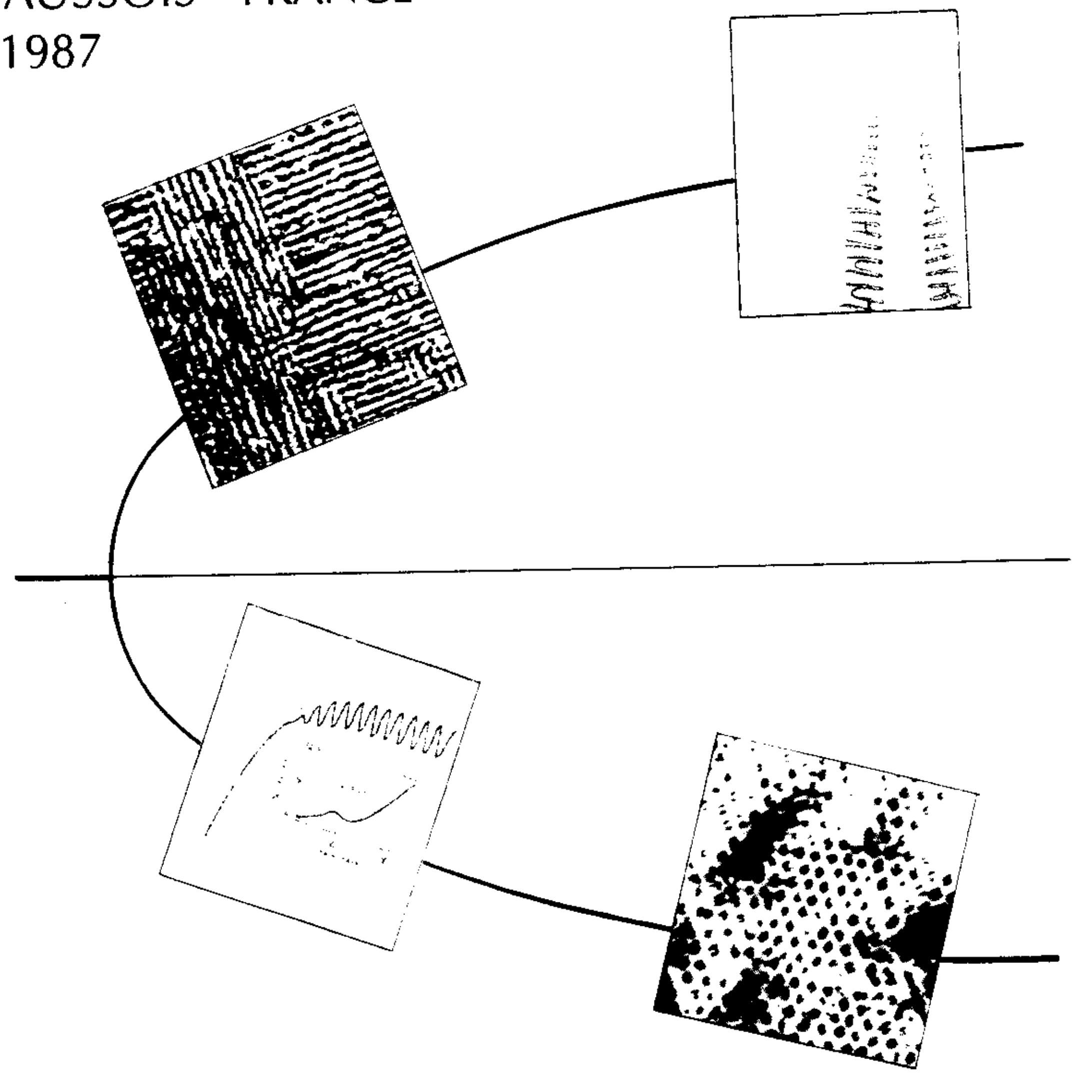

Editors: L. Kubin
G. Martin

TRANS TECH PUBLICATIONS

Solid State Phenomena Vol.3&4 (1988) pp. 357-368

DISLOCATION DYNAMICS AND COOPERATIVE BEHAVIOUR OF DISLOCATIONS

G. Ananthakrishna

Indira Gandhi Centre for Atomic Research
Kalpakkam 603 102, India

ABSTRACT

We present a theoretical model of repeated yielding which reproduces many experimentally observed features apart from demonstrating how the temporal behaviour emerges as a natural consequence of the cooperative behaviour of defects. The starting point for building such a model is our earlier work on a statistical description of dislocation dynamics which explains creep in simple materials. The model leads to an alternate but equivalent description which allows us to quantify the mobile dislocation density in terms of a coupled set of equations for the mobile and the immobile components. We then include another type of dislocation and some transformations between them. This leads to a coupled set of nonlinear differential equations for the three dislocation densities. We show that for a range of values of the rate constants, limit cycle solutions are exhibited leading to jumps on creep curve. Approximate closed form solutions are also obtained. The model is extended to the constant strain rate case by coupling the above equations to the machine equation. The temporal ordering of repeated yielding naturally follows. Several such features as bounds on the strain rate, bounds on the concentration of solute atoms, the negative strain rate dependence of the flow stress, the dependence of the amplitude on the strain rate, strain etc., emerge from the model. The model also exhibits period doubling bifurcation with an exponent value same as that for the quadratic map. Finally we report the effect fluctuations during a single yield drop.

1. INTRODUCTION

Repeated yielding (RY) of materials and their counterparts in creep and constant stress rate tests have long been addressed as some kind of instability. However it is only in the last six years or so the word instability has been brought to sharp focus by the use of dynamical systems method which quantifies it as a bifurcation. A complete description of the phenomenon which includes the initiation and propagation of the bands during RY appears to be difficult even after a first modest attempt was undertaken several years ago [1,2] wherein the spatial inhomogeneity was ignored, and only temporal oscillatory state was sought to be described. The analysis did demonstrate that the oscillatory state was the result of a Hopf bifurcation beyond a stability limit in the control parameter (the strain rate) [3-5]. It was an important step, since the phenomena was brought into the general framework of nonequilibrium phase transitions and pattern formation. Attempts by several authors that followed in respect to low temperature repeated yielding [6] and formation of cell structure during fatigue [7] did demonstrate that other forms of ordering (used in a general sense of even temporal ordering) could be explained within the general framework of bifurcation theory. Several other papers in this conference substantiate the power of the dynamical systems method [8-10].

There have been a number of phenomenological treatments [11-14] which have contributed immensely to the general understanding of RY. The best known model is Cottrell's dynamic strain ageing model or its improved versions. In these models expressions are derived for such quantities as the critical strain rate, the dependence of the flow stress on strain rate etc. However, little attention has been paid to relating these quantities to the basic dislocation mechanisms. Further, no attempt has been made to investigate how the temporal behaviour of repeated yielding could arise as natural consequence of the basic dislocation mechanisms.

In the following I outline our particular efforts to understand the macroscopic manifestations of dislocation interactions [15-17] and the consequent emergence of temporal ordering [1-5].

2. A STATISTICAL THEORY OF DISLOCATION DYNAMICS

The starting point for our study is a statistical theory of dislocation dynamics which happens to be a natural starting point for various reasons. To motivate this consider the conceptual difficulty in dealing with a constant strain rate experiment. From the physicists point of view we are seeking to determine the stress developed in the sample for which we have imposed a predetermined response. This is to be contrasted with what we normally do in physics wherein we look for the response of the system when a force is applied. From this point of veiw the equivalent experimental situation to consider is the creep test, wherein the instabilities will manifest as steps on creep curve. Further since our intention is to make contact with macroscopic properties to the basic dislocation mechanisms, we consider a simple situation of the dynamics of dislocations in simple materials like LiF [15,17-19]. The hope is that we will be able to see the macroscopic manifestations of dislocation interactions which should guide us in modelling the more complicated situation of RY.

The fundamental quantity we introduce is the probability density $\rho(v,t)$ of dislocation line segments having a velocity v. The continuity equation for ρ is

$$\frac{\partial \rho(v,t)}{\partial t} + \frac{\partial J}{\partial v} = S \tag{1}$$

where

$$J = -\left(\frac{B_0}{M} v - \frac{b_0 \sigma_a}{m} - \frac{Q}{M}\frac{\partial}{\partial v}\right)\rho(v,t) = -\left(\beta v - f + q\,\frac{\partial}{\partial v}\right)\rho(v,t) \tag{1a}$$

is the current. (Here b_0 is the Burges vector, B_c is the drag force, $b_0\sigma_a$ is the force per unit length on a dislocation, M is the mass of a dislocation of a unit length.) The source term has the following contributions:

$$S = (-\alpha + \theta v)\rho(v,t) - \mu\int_{-\alpha}^{\infty}\rho(v-v')\,\rho(v')\,dv' + h\int_{-\infty}^{\infty}\rho(v-v')\frac{\partial \rho(v')}{\partial v'}dv' \tag{1b}$$

The first term corresponds to a loss due to stopping of dislocations at precipitates, grain boundaries etc., the second term is the production of dislocations due to the cross glide [18,19], the third and the fourth terms correspond to the interaction of dislocations resulting in the formation of dipoles etc. (arising out of the reduction of the velocities). For more details we refer the reader to the original paper [15].

This approach unifies several phenomenologocal relations introduced in the literature in different contexts [19]. The following relations follow immediately (see [19])

$$\frac{dN}{dt} = (-\alpha + \theta V)N - \mu N^2 \tag{2}$$

and

$$M\frac{dV}{dt} = -B_0 V + b_0\sigma_a - hNM \tag{3}$$

where N is the total dislocation density and V is the average velocity $\langle v\rangle$. The second relation gives an expression for the back stress σ_i in the steady state:

$$V = b_0\sigma_a/B_0 = b_0(\sigma_a - \sigma_i)/B_0 = b_0(\sigma_a - hNM/b_0)/B_0 \tag{4}$$

These two equations are adequate to obtain a creep law. This creep law is similar to that obtained by Webster (see [19]). The only adjustable quantity is h. Even this is not arbitrary since it must be compatible with the velocity reduction due to hardening [19]. The calculated creep curve fits the experiments very well as can be seen in figure 1.

A few remarks of technical nature may be in order. Although, equation (1) appears to be complicated, it is possible to obtain exact expressions for the first four cumulants given by

$$\begin{aligned} k_1 &= \langle v\rangle = V = (f - hN)/\beta \\ k_2 &= \langle v^2\rangle - V^2 = (2q - hNV)/\beta \\ k_3 &= -hN\langle v^2\rangle/\beta \\ k_4 &= -hN\langle v^3\rangle/\beta \end{aligned} \tag{5}$$

It appears plaussible that k_n, $n \geq 3$ may have the same behaviour as k_3 and k_4 i.e. $k_n = -(h/\beta)\, N \langle v^{n-1} \rangle$. If we assume this, it is possible to obtain closed form expressions for the characteristic function of the distribution [16]. One interesting aspect of this distribution is that for appropriate choice of parameters, the distribution function can become sharp i.e. $k_2 \rightarrow 0$. This feature of the distribution function may have some relevance in the problem of the formation of void lattice.

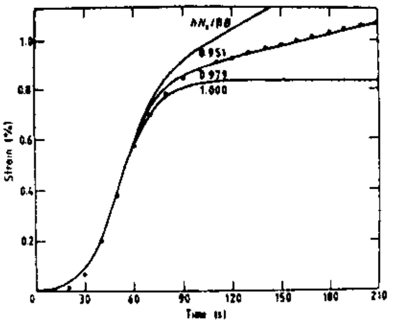

Fig.1 Theoretical creep curve:-- Experimental points: •

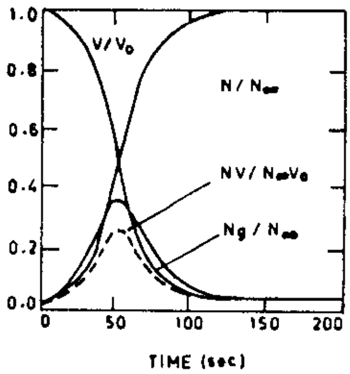

Fig.2 Form of V ,N, NV and N_g

The above description in terms of a distribution function gives a natural tool to quantify mobile dislocation density. Formally writing $\rho(v,t) = \rho_s(v,t) + \rho_g(v,t)$ where the subscipts stand for the immobile and the mobile respectively, we obtain $NV = N_s V_s + N_g V_g$, where $\langle v \rangle_{s,g} = V_{s,g}$. Since V_s is expected to be small, we have, $NV \simeq N_g V_g$. By reformulating the above theory to account for the production of dipoles (see [17] for details), we obtain

$$\dot{N} = \theta V N - \mu N^2 \tag{6}$$

$$\dot{N}_g = k \mu N^2 - \mu N N_g \tag{7}$$

where $N_g = N - N_s$ is the density of dipoles and k is a constant. These equations can be solved to obtain the creep curve which again fits the data equally well as the earlier description (in terms of N and V). The parameter $k = h\theta/\beta$. Thus, the two descriptions are equivalent. In the later, the entire time dependence of the flow is controlled by the mobile dislocation density N_g and V_g is nearly constant. To the best of authors knowledge this was the first attempt to obtain the mobile dislocation density in dynamic balance during creep [17]. The procedure adapted is not restrictive and can be generalized to other more complicated situations if the governing mechanisms are known. The forms of N, V and their product NV and N_g are shown in figure 2. It is clear that NV has the same form as N_g.

3. A MODEL FOR STEPS ON CREEP CURVE

Coupled set of nonlinear equations such as equations (6) and (7) can lead to oscillatory solutions for suitable choice of the parameters [20-22], although in its present form they do not support oscillatory solutions. Under such conditions a stepped response during creep will be observed [23-28]. It is then very suggestive to enlarge the above model to account for other mechanisms and look for oscillatory solutions. The above model could also be thought of as a transformation between the mobile (denoted by g) and the immobile dislocations (s). In the present case, we introduce a third species of dislocations (denoted by i) which is surrounded by solute atoms [11]. These dislocations are much slower than the mobile ones, ultimately becoming immobile.

Let N_g, N_s and N_i denote the densities of g, s and i species respectively. The rate equations for these quantities are (a dot denotes the time derivative):

$$\dot{N}_g = \theta V_g N_g - \mu N_g^2 - \mu N_g N_s + \lambda N_s - \alpha N_g \qquad (8)$$

$$\dot{N}_s = k \mu N_g^2 - \mu N_g N_s - \lambda N_s + \alpha' N_i \qquad (9)$$

$$\dot{N}_i = \alpha N_g - \alpha' N_i \qquad (10)$$

We assume that μ, λ, α, α', θ and k are constants for a given stress at a given temperature. The first two terms in the equation (8) has been defined earlier except that the rate constant for the second term has been taken to be $(1-k)\mu$. The third term corresponds to the annihilation of a mobile dislocation with an immobile one and the last term arises from solute atoms gathering around dislocations. Once a certain amount of solute atoms gather around a moving dislocation, its mobility is reduced, and it should be considered as a type i dislocation (hence the source term αN_g in equation (10)). As the size of the solute atom cloud increases, the dislocation eventually becomes immobile (hence the source term $\alpha' N_i$ in equation (9)). The terms λN_s comes from the (thermal or athermal) activation of immobile dislocations. The parameter α is expected to depend on the diffusion constant of the solute atoms, their concentration and the velocity of dislocations of type i. The parameter α' is the rate of immobilization, and hence should be expected to depend on the critical velocity (k is a parameter close to unity).

It is convenient to rewrite equations (8) to (10) in a dimensionless form by setting

$$x = (\mu/\lambda) N_g \, , \; y = (\mu/\theta V_g) N_s \, , \; Z = (\mu \alpha'/\lambda \alpha) N_i \qquad (11)$$

$$\tau = \theta V_g t \, , \; a = \alpha/\theta V_g \, , \; b = \lambda/\theta V_g \, , \; c = \alpha'/\theta V_g$$

Then

$$dx/d\tau = (1-a)x - b x^2 - x y + y \qquad (12)$$

$$dy/d\tau = b(kbx^2 - xy - y + az) \quad (13)$$

$$dz/d\tau = c(x - z) \quad (14)$$

Equations (12-14) form a coupled set of nonlinear equations. Under well known conditions [20], these admit periodic solutions called limit cycles for a certain range of values of the parameters a,b,c and k. The stability analysis can be carried out to determine the boundary of instability domain in the parameter space. Further it can be shown that the system of equations admits Hopf bifurcation, leading to a limit cycle solution. It is also possible to obtain approximate closed form solutions by adiabatically eliminating the fast mode x. Thus, we would have two null clines $z_1 = z(y)$ and $z_2 = x(y)$. These intersect in the negative slope region only for the values of parameters in the instability domain [1,2]. A plot of the null clines is shown in figure 3. It is possible to obtain expressions for steps on the creep curve (both numerically and analytically). Several features that we obtain such as the steps appearing in steady state creep situation [27,28], the monotonic dependence of the step hight on and the weak dependence of the period on [26] are consistent with our theory. A number of other features also follow. For details we refer the reader to reference [1] and [2] except to mention here that there are upper and lower bounds on the concentration of solute atoms (α) and temperature T ($V_g = V_g(T)$) over which the steps are observed. A typical such creep curve is shown in figure 4.

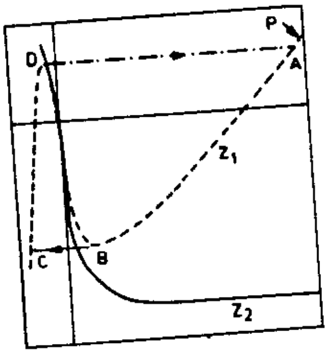

Fig.3 Null clines $z_1(y)$ and $z_2(y)$.

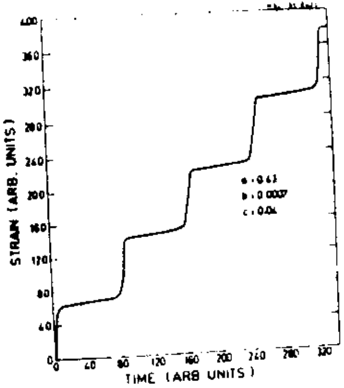

Fig.4 Stepped nature of the creep curve

4. REPEATED YIELD DROP BEHAVIOUR

Our model can be extended to a constant strain rate experiment by augmenting equations (8-10) with the machine equation representing the load sensed by the load cell, namely

$$\dot{\sigma}_a = k[\dot{\varepsilon} - b_0 N_g V_g(\sigma^*)] \quad (15)$$

Here $\dot{\varepsilon}$ is the imposed strain rate, K is the effective compliance, and σ^* is the effective stress. The second term on the right in equation (15) is the plastic strain rate $\dot{\varepsilon}_p$. We assume the power law $V_g = V_0(\sigma^*/\sigma_0)^m$, with $\sigma^* = \sigma_a - HN^{1/2}$, where H is a constant characteristic of hardening and m is a velocity exponent. Following a procedure similar to that of the earlier section, it can be shown that there is a domain in the space of the relevant parameters for which limit cycle solutions exist. Choosing values of the parameters in the domain of instability so as to be consistent with the expected values of the dislocation densities and the yield drops, numerical solutions of the system of equations may be obtained, and various characteristic features of the RY exhibited may be studied. These appear to be generally consistent with the experimental results. We list these salient features: (a) There is a range of $\dot{\varepsilon}$ over which serrations are seen. (b) The model exhibits the negative strain rate behaviour of the flow stress at a fixed value of the plastic strain. The inset in figure 5 shows a typical plot of σ_a vs $\dot{\varepsilon}_p$, with a minimum of σ_a at a point $\dot{\varepsilon}_p = \dot{\varepsilon}_{min}$. Curves corresponding to larger ε_p are displaced successively upwards. This feature has been both theoretically [13] and experimentally verified [12]. (c) Figure 5 shows a typical plot of serrated yielding. The serrations are asymptotically periodic. From a strain rate change test [29] it is found that beyond $\dot{\varepsilon}_p$ the serrations are of type B. (d) The amplitude of the serration increases upto $\dot{\varepsilon}_{min}$ and decreases thereafter. (e) The amplitude increases and saturates as a function of ε, consistent with experiments [30]. (f) There are upper and lower bounds on the parameter α of equation (8) within which serrated yielding occurs. Since α depends on the concentration of solute atoms, this implies that there is a range of the solute atom concentration in which the phenomenon occurs. (g) ε_c (the critical strain), as a function of $\dot{\varepsilon}$, first decreases and then increases [30]. (h) Beyond the range of $\dot{\varepsilon}$ where serrated yielding occurs, the 'normal' behaviour of $\sigma_a(\dot{\varepsilon})$ is resumed. (For details see [3]).

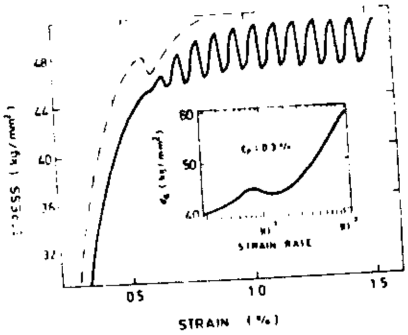

Fig.5 The theoretically obtained multiple yield drop plot. The Inset shows σ_a vs $\dot{\varepsilon}_p$

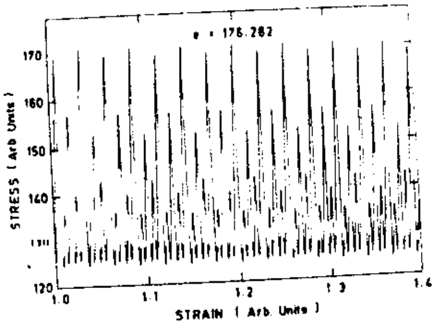

Fig. 6 Period 2^3 cycle for e = 176.282

It should be pointed out that so far there has not been any attempt to derive the negative strain rate behaviour of the flow stress (which is crucial for any meaningful description of the phenomenon) starting from dislocation interactions. In the existing theories this is either assumed [13] or derived [14] through a phenomenological treatment of waiting times, involving in any case, only individual dislocations. In contrast, this property emerges naturally in the present model from a consideration of dislocation interactions.

We have shown that the new temporal order represented by serrated yielding is the consequence of a bifurcation from a temporally homogeneous steady state plastic flow beyond some critical value of the parameters. This order is the result of a balance between the energy input (in the form of dislocation multiplication) and dissipation (annihilation, immobilisation and other processes). The phenomenon is obviously a far from equilibrium situation and is an example of a self organized system [21, 22].

5. CHAOTIC FLOW

We now turn to the chaotic flow exhibited by our model over a certain range of a drive parameter, the applied strain rate. (There is also some experimental evidence for such a flow [4]). This adds to the growing list of models and physical situations exhibiting chaos [31-33]. The model has an infinite sequence of period-doubling bufurcation eventually leading to chaos. The region over which chaos is exhibited is very small compared to the range of over which RY is seen. We have calculated the value of the associated exponent and found it to be the same as the exponent for the quadratic map. We have also obtained the associated one-dimensional map. As the parameter of interest is the applied strain rate $\dot{\epsilon}$, we fix the values of all the other parameters within the instability region and study the bifurcation sequence with respect to the parameter $e = (\dot{\epsilon} r / V_0 b_0)$. The region where the period doubling bifurcation occurs is small, and is located near the upper end of the range of e (the dimensionless strain rate) over which RY is observed. For the chosen values of the parameters, the first bifurcation from the periodic state with period T to a state with a period 2T occurs at $e_1 = 159.98444$, while the successive bifurcation to states with period 4T, 8T,..., occur at $e_2 = 173.7178$, $e_3 = 175.8974$, ... The exponents $\delta_n = \lim(e_n - e_{n-1})/(e_{n+1} - e_n)$ appears to be very close to that obtained by for the quadratic map [34,35]. The estimated value of e_∞ is 176.4669, beyond which we find chaotic motion. Figures 6 and 7 show the variation of the stress ϕ with time (equivalently, the strain) for $e = 174.697$ (motion with period 8T) and $e = 178.205$ (chaotic motion) respectively. A log-log plot of the projection of the strange attractor in the $N - \phi$ plane is shown in figure 8. The associated one-dimensional map a smooth rounded maximum similar to the quadratic map except that it is skewed [4].

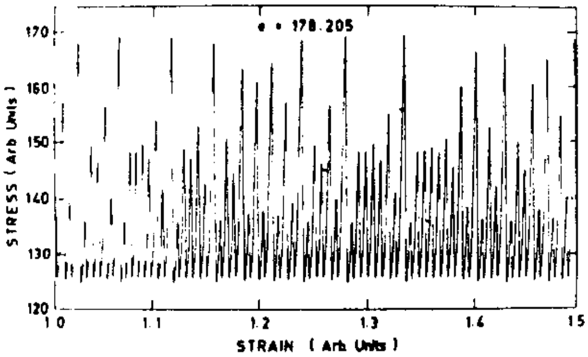

Fig.7 Stress-strain curve for the chaotic state.

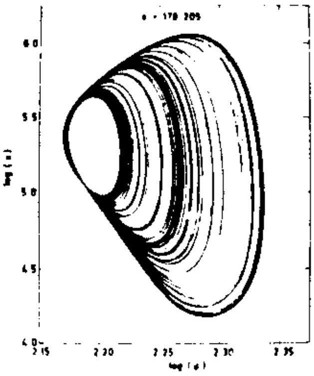

Fig.8 Log-log plot of the projection of the strange attractor inthe N-ϕ plane.

6. EFFECT OF FLUCTUATIONS

Finally we briefly discuss the effect of fluctuations during a single yield drop. (Effect of fluctuations on multiple yield drops has also been analysed [5].) The particular example considered here represents the plastic flow in materials like GeSi [16]. The equations for the density of dislocations N and the stress σ_a are

$$dN/dt = a_1 \sigma_a N - b_1 N^{3/2} \tag{16}$$

$$d\sigma_a/dt = k[\dot{\varepsilon} - b_1 \sigma_a N + c_1 N^{3/2}] \tag{17}$$

where a_1, b_1 and c_1 are constants. To consider the effect of fluctuations, it is conventional to add a noise term whose statistical properties are defined, normally chosen as a white noise [37]. This is done after transforming the first equation to $x = N^{1/2}$ so that we have an analytic variable x whose fluctuations will be determined. The analysis is carried out using both Gaussian decoupling and Monte Carlo methods. For details we refer the reader to the original paper [38]. Here we shall present the principal results and discuss the implications. The average values of σ_a and x are well reproduced (i.e. their behaviour is the same as that obtained from equations (16-17)) which is as should be expected. However, there are anomalous fluctuations in x and y , whose values peak exactly at the value of the yield drop. Figures (9) and (10) show fluctuations in x and y as a function of time (or strain). Anomalous fluctuations manifest in all systems which pass from a unstable state to a relatively stable state. Such anomalous fluctuations should be seen in scattering experiments. Indeed the attenuation of ultrasonic waves during an yield drop experiment does show a marked behaviour [38]. Our interpretation is that this is a consequence of anomalous fluctuations and not merely due to the link length change as has been interpreted earlier [39]. A detailed calculation to express the attenuation in terms of fluctuations in the number of dislocations is in progress.

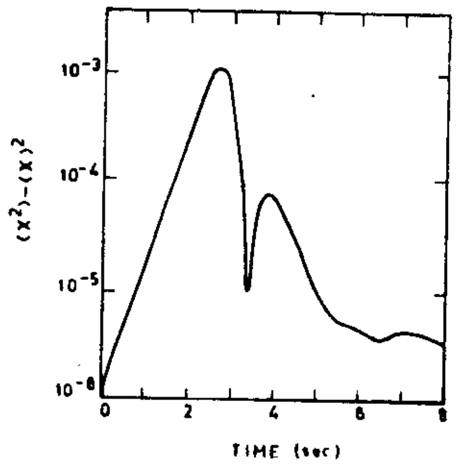

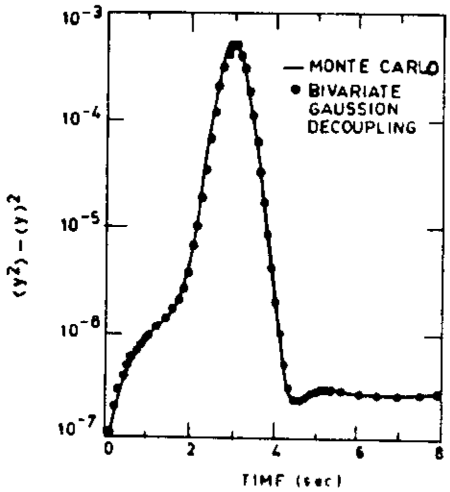

Fig.9 A plot of fluctuations in x. Note the magnitude of fluctuations is four orders at the yield point.

Fig.10 Fluctuations in stress. Again the fluctuations are large and peak at the yield drop

In summary, a need to understand the RY as arising due to dislocation interactions initiated us to investigate creep in simple materials from a dislocation dynamical model. This model led us to quantify the mobile dislocation density which in turn led us to a model for jumps on creep curve. A straight forward extention of this model to the costant strain rate case explains a large number of quantitative features of RY. The model is shown to exhibit chaotic flow as well. We have also breifly presented our analysis on the effect of fluctuations.

[1] Ananthakrishna, G. and Sahoo D.: J.Phys., 1981, D14, 2081
[2] Valsakumar, M.C. and Ananthakrishna, G.: J. Phys., 1983, D16, 1055
[3] Ananthakrishna, G. and Valsakumar, M.C.: J. Phys., 1982, D15, L171
[4] Ananthakrishna, G. and Valsakumar, M.C.: Phys. Lett., 1983, A95, 69
[5] Ananthakrishna, G.: Bull. Mater. Sci., 1984, 6, 665
[6] Kubin, L.P., Estrin, Y. and Spiesser, Ph.: Res. Mechanica, 1984, 10, 25
[7] Walgraef, D. and Aifantis, E.: Int. J. Energy Sci., 1985, 23, 1351, 1359, 1365; Aifantis, E.: This volume
[8] Estrin, Y.: This volume and references therein
[9] Brechet, Y. and Louchet, F.: This volume

[10] Lepinoux, J. and Kubin, L.P.: This volume

[11] Cottrell, A.H.: Phil. Mag., 1953, 44, 829

[12] Bodner, S.R. and Rosen, A.: J. Mech. Phys. Solids, 1967, 15, 63

[13] Penning, P.: Acta Metall., 1972, 20, 1169

[14] van den Benkel, A.: Phys. Stat. Sol., 1975, A30, 197; Acta Metall., 1980, 20, 965

[15] Ananthakrishna, G. and Sahoo, D.: J. Phys., 1981, D14, 699

[16] Ananthakrishna, G.: J. Phys., 1981, D14, 2091; 1982, D15, 77

[17] Sahoo, D. and Ananthakrishna, G.: J. Phys., 1982, D15, 1439

[18] Gilman, J.J. and Johnston, W.G.: J. Appl. Phys., 1960, 31, 687

[19] Gilman, J.J.: Micromechanics of Flow in Solids (New York: McGraw-Hill) 1969

[20] Minorsky, N.: Nonlinear Oscillations (New Jersey: Van Nortrand) 1962

[21] Nicolis, G. and Prigogine, I.: Self Organization in Non-Equilibrium Systems (New York: Wiley) 1977

[22] Haken, H.: Synergetics (Berlin: Springer-Verlag) 1977

[23] Ardley, G.W. and Cottrell, A.H.: Proc. R. Soc., 1953, A219, 328

[24] Navratil, V., Hammersky, M. and Blazkova.: Czech. J. Phys., 1974, B24, 907

[25] Stejskalova, V., Hammersky, M., Luckac, P., Vostry, P. and Sprucil, B.: Czech. J. Phys., 1981, B31, 195

[26] Zagarukuyko, L.N., Ostasky, A.L. and Soldatov, V.P., Phys. Met. Metallogr., 1977, 43, 156

[27] Da Silveira, T.L. and Monterio, S.N.: Met. Trans., 1979, A10, 1745

[28] Lubahn, J.D. and Felgar, R.P.: Plasticity and Creep of Metals (New York: John Wiley) 1961

[29] Wijler, A. and van Westrum, S.: Scr. Metall., 1971, 5, 31

[30] McCormic, P.G.: Acta Metall., 1971, 21, 463

[31] Ott, E.: Rev. Mod. Phys., 1981, 53, 655

[32] Eckmann, J.P.: Rev. Mod. Phys., 1981, 53, 643

[33] Bai-Lin, H.: Chaos (Singapore: World Scientific) 1985

[34] Grossman, S. and Thomae, S.: Z. Naturforsch., 1977, 32a, 1353

[35] Feigenbaum, M.J.: J. Stat. Phys., 1978, 19, 25

[36] Valsakumar, M.C., Murthy, K.P.N. and Ananthakrishna, G.: J. Stat. Phys., 1983, 30, 637

[37] Van Kampen, N.G.: Stochastic Processes in Physics and Chemistry (Amsterdam: North Holland) 1981

[38] Baldev Raj, et al., 1987, to be published

[39] Higgens, F.P. and Carpenter, S.H.: Acta Metall., 1978, 26, 133